Cerebral Cortex, March 2017;27:1931–1943

doi:10.1093/cercor/bhw021
Advance Access Publication Date: 27 February 2016
Original Article

ORIGINAL ARTICLE

The Number of Parvalbumin-Expressing Interneurons Is Decreased in the Prefrontal Cortex in Autism

Ezzat Hashemi[1,3], Jeanelle Ariza[1,3], Haille Rogers[1,3], Stephen C. Noctor[2,4] and Verónica Martínez-Cerdeño[1,3,4]

[1]Department of Pathology and Laboratory Medicine, [2]Department of Psychiatry and Behavioral Sciences, UC Davis, Sacramento, CA, USA, [3]Institute for Pediatric Regenerative Medicine and Shriners Hospitals for Children Northern California, Sacramento, CA, USA and [4]MIND Institute, UC Davis School of Medicine, Sacramento, CA, USA

Address correspondence to Verónica Martínez-Cerdeño, 2425 Stockton Boulevard, Sacramento, CA 95817, USA. Email: vmartinezcerdeno@ucdavis.edu

Abstract

The cognitive phenotype of autism has been correlated with an altered balance of excitation to inhibition in the cerebral cortex, which could result from a change in the number, function, or morphology of GABA-expressing interneurons. The number of GABAergic interneuron subtypes has not been quantified in the autistic cerebral cortex. We classified interneurons into 3 subpopulations based on expression of the calcium-binding proteins parvalbumin, calbindin, or calretinin. We quantified the number of each interneuron subtype in postmortem neocortical tissue from 11 autistic cases and 10 control cases. Prefrontal Brodmann Areas (BA) BA46, BA47, and BA9 in autism and age-matched controls were analyzed by blinded researchers. We show that the number of parvalbumin+ interneurons in these 3 cortical areas—BA46, BA47, and BA9—is significantly reduced in autism compared with controls. The number of calbindin+ and calretinin+ interneurons did not differ in the cortical areas examined. Parvalbumin+ interneurons are fast-spiking cells that synchronize the activity of pyramidal cells through perisomatic and axo-axonic inhibition. The reduced number of parvalbumin+ interneurons could disrupt the balance of excitation/inhibition and alter gamma wave oscillations in the cerebral cortex of autistic subjects. These data will allow development of novel treatments specifically targeting parvalbumin interneurons.

Key words: autism, basket cells, chandelier cells, interneurons, parvalbumin, prefrontal cortex

Introduction

Autism spectrum disorders (ASDs) are defined by a pattern of qualitative abnormalities in reciprocal social interaction, communication, and repetitive interest and behavior. Recent estimates indicate that 1 in 68 children in the USA suffer from ASD (Baio 2012). ASDs occur in all racial, ethnic, and socioeconomic groups, yet on average are 4 to 5 times more likely to occur in boys than in girls. Classical autism is the most common condition among ASDs. Autism symptoms cover a wide spectrum, ranging from individuals with severe impairments who may be silent and mentally disabled, to high functioning individuals who suffer from mild impairments in social approach and communication. The wide range of manifestations of autism likely arises from distinct etiologies. While the etiology of autism and ASD remains poorly understood, it is commonly thought to result from genetic, environmental, and/or immune factors (Mandy 2016; Martinez-Cerdeno 2016; Schaefer 2016).

Altered functioning of several areas of the brain is thought to underlie the social and cognitive phenotype in autism. Identified brain regions include the prefrontal and temporal cerebral cortex, hippocampus, amygdala, striatum, and cerebellum, among others. Within the prefrontal cortex (PFC) areas implicated in autism include: BA9—involved in working and spatial memory, verbal fluency, auditory and verbal attention, and attributing

intention; BA46—also known as dorsolateral PFC, which plays a role in attention and working memory; and BA47—which is involved in processing syntax in oral and sign languages. The cognitive functions served by areas BA46, BA47, and BA9 are impaired in autism (Romanski 2007; Dumontheil et al. 2008; Shalom 2009; Teffer and Semendeferi 2012; Dixon and Christoff 2014; Dumontheil 2014; Jeon 2014). Whether and how cytoarchitecture in these regions of the brain is altered in autism, particularly the cortical areas, is not well understood. Possible alterations in cortical structures that underlie the autism phenotype range from impaired formation and functioning of synapses, to altered numbers of neurons and/or glial cells. In agreement with the latter concept, early brain overgrowth in autism has been theorized to result from alteration in cellular numbers in the cerebral cortex (Courchesne et al. 2011).

EEG recordings from the cerebral cortex of autistic patients exhibit an alteration of induced gamma activity patterns (Belmonte and Yurgelun-Todd 2003; Brown et al. 2005; Oberman et al. 2005; Orekhova et al. 2007; Cohen et al. 2009; Milne et al. 2009; Russo et al. 2009; Thatcher et al. 2009). The gamma activity pattern in autistic subjects indicates an imbalance in the ratio of excitation/inhibition in the cerebral cortex. Published evidence suggests that this ratio may be pushed in either direction—either too much excitation or too much inhibition—depending on underlying cause(s). For example, data indicating that a decreased ratio of excitation/inhibition (increased inhibition) underlies the cognitive phenotype in autism have been reported in a mouse model of Rett Syndrome in mice lacking MeCP2 (Dani et al. 2005), and in mice that express the human allele of Neuroligin3, a gene defect associated with some cases of autism (Tabuchi et al. 2007). On the other hand, evidence that an increased ratio of excitation/inhibition (increased excitation) underlies the cognitive phenotype of autism is supported by the prevalence of epilepsy in autistic patients (Francis et al. 2013). The cause of these functional changes is not well understood. Possible mechanisms that could alter the balance of excitation/inhibition include a change in the number of excitatory pyramidal neurons and/or inhibitory interneurons in discrete regions of the cerebral cortex. Altered numbers of a given cortical neuron subtype in a specific region of the cortex could alter the pattern of cortico-cortical connections and produce disturbances in cognitive functioning (Rubenstein and Merzenich 2003; Polleux and Lauder 2004; Cline 2005). Indeed, animal models that exhibit an imbalance in the ratio of pyramidal neurons to interneurons in the neocortex show behavioral features that are consistent with autism, including reduced social interaction and increased anxiety (Helmeke et al. 2008).

Several studies have examined the number of cells in various regions of the autistic brain, including the number of pyramidal neurons and von Economo neurons in prefrontal, temporal, and fusiform cortical areas. Some studies have found an altered number of pyramidal neurons or von Economo neurons in the cerebral cortex, while other studies have not reported abnormalities (Casanova et al. 2002, 2010; Mukaetova-Ladinska et al. 2004; Kennedy et al. 2007; van Kooten et al. 2008; Courchesne et al. 2011; Santos et al. 2011; Camacho et al. 2014; Uppal et al. 2014; Kim et al. 2015). An alteration in the number of neurons in other brain structures, including the cerebellum and amygdala, has also been correlated with autism (Fatemi et al. 2002; Schumann and Amaral 2005, 2006; Whitney et al. 2008, 2009; Skefos et al. 2014; Wegiel et al. 2014). However, to the best of our knowledge, there has not yet been a study specifically designed to quantify the number of interneurons, and interneuron subtypes, in the cerebral cortex in autism. An alteration in the number of interneurons, or interneuron subtypes, could alter the balance of excitation/inhibition in the cerebral cortex. Supporting this concept, mice with null mutations in the Dlx1 gene show a loss of specific interneuron subtypes and have reduced inhibition and epilepsy—symptoms that are commonly seen in autism (Cobos et al. 2005; Levisohn 2007; Rubenstein 2010).

Interneurons in the cortex exhibit a wide variety of morphological, physiological and molecular characteristics. In postmortem tissue interneurons can be classified on the basis of the expression of specific molecular markers. For example, distinct groups of interneurons can be identified using 5 markers specific for parvalbumin (PV), somatostatin (SOM), neuropeptide Y (NPY), cholecystokinin, and vasoactive intestinal peptide (VIP). This approach identifies the following subgroups of interneurons: 1) PV+ cells, such as chandelier and basket cells; 2) SOM+ cells, such as Martinotti cells; 3) cells that express NPY but not SOM; 4) cells that express VIP; and 5) cells that express cholecystokinin but not SOM or VIP. These 5 interneuron subtypes can be further subdivided based on a variety of characteristics (see DeFelipe et al. 2014). An alternative approach classifies interneurons into 3 main subtypes based on their expression of the proteins parvalbumin (PV), calbindin (CB), and calretinin (CR), (Hof et al. 1999). These markers identify 3 subpopulations of distinct interneurons that are defined by their morphology, laminar distribution in the cerebral cortex, physiological properties, connectivity, and developmental origin (Kubota et al. 1994; Cauli et al. 1997; del Rio and DeFelipe 1997; DeFelipe 1997; Leuba and Saini 1997; Hof et al. 1999; DeFelipe et al. 2013).

Neurons immunoreactive for PV are mostly chandelier cells and large basket cells; those immunoreactive for CR are bipolar cells, double bouquet cells, and Cajal–Retzius cells; and those immunoreactive for CB are double bouquet cells. In addition, some CB+ cells have been identified as neurogliaform cells and others as Martinotti cells in the monkey PFC (Conde et al. 1994; DeFelipe 1997). The approach of classifying cortical interneurons into 3 subsets based on PV, CR, or CB expression does not exclude interneurons that express other interneuron markers such as SOM, NPY, or VIP. For example, SOM+ interneurons would be accounted for primarily within the CB+ subset and to a lesser degree within the PV+ and CR+ subsets (Kubota et al. 1994; Kawaguchi and Kubota 1997; Nassar et al. 2015). Previous studies have used this method to comprehensively identify interneuron subpopulations in the cortex of mammalian species (Hof et al. 1999) and to identify interneuron subpopulations in human cortical tissue obtained from patients with certain diseases. For example, Kuchukhidze and colleagues quantified the number of PV+, CB+, and CR+ cells in patients with cortical dysplasia and reported an increased number of PV+ cells in the lateral temporal cortex (Kuchukhidze et al. 2015). To investigate whether there are changes in the number or proportion of interneuron subpopulations in the cerebral cortex in autism, we chose to collect data using the more straightforward and easier to implement approach that classifies interneurons based on their expression of the PV, CR, and CB calcium-sequestering proteins. Determining whether there is a change in the number of interneurons or interneuron subtypes in autism is a fundamental step that will shed light on the origins of the altered excitation/inhibition balance in the autistic cerebral cortex and, this in turn, may yield new therapeutic interventions.

Results

We identified prefrontal Brodmann areas BA9, BA46, and BA47 in cerebro-cortical tissue samples obtained from 11 autism and 10 control, age-matched cases (Table 1). The tissue was obtained

Table1 Clinical characteristics of postmortem cases, including sex, age, diagnosis, postmortem interval (PMI), brain mass, hemisphere, cause of death, the presence of seizures or mental retardation, and repetitive, verbal, non-verbal, and social scores for the autism cases

Case ID	Sex	Age	Diagnosis	PMI (hours)	Brain mass (g)	Hemisphere	Cause of death	Seizure	Mental retardation	Rept. score	Verbal score	Nonverbal score	Social score
UCD-13AP86	M	6	Control	NK	NK	NK	NK	NA	NA	NA	NA	NA	NA
AN07444 (B7387)	M	17	Control	30.75	1460	Right	Asphyxia	NA	NA	NA	NA	NA	NA
AN00544 (B6951)	M	17	Control	28.92	1250	Left	NK	NA	NA	NA	NA	NA	NA
AN19760 (B5873)	M	28	Control	23.25	1580	Right	NK	NA	NA	NA	NA	NA	NA
AN12137 (B5352)	M	31	Control	32.92	1810	Right	Asphyxia	NA	NA	NA	NA	NA	NA
AN15566 (B6316)	F	32	Control	28.92	1360	Right	NK	NA	NA	NA	NA	NA	NA
AN05475 (B7561)	M	39	Control	NK	1350	Right	Cardiac arrest	NA	NA	NA	NA	NA	NA
AN17868 (B5812)	M	46	Control	18.78	1588	Right	Cardiac arrest	NA	NA	NA	NA	NA	NA
AN19442 (B6259)	M	50	Control	20.4	1740	Right	NK	NA	NA	NA	NA	NA	NA
AN13295 (B6860)	M	56	Control	22.12	1370	Left	NK	NA	NA	NA	NA	NA	NA
AN03221 (B6242)	M	7	Autism	11.42	1560	NK	Drowning	No	No	8	16	NA	27
AN01293 (B6349)	M	9	Autism	4.41	1690	Left	Cardiac arrest	No	Yes	5	NA	12	26
AN00394 (B4323)	M	14	Autism	10.3	1615	NK	Cardiac arrest	No	No	NK	NK	NK	NK
An02736 (B5891)	M	15	Autism	2.5	1390	Right	Aspiration	Yes	No	NK	NK	NK	NK
AN00764 (B5144)	M	20	Autism	23.66	1144	Right	Accident	No	No	NK	NK	NK	NK
AN00493 (B5000)	M	27	Autism	8.3	1575	Right	Drowning	No	Yes	NK	NK	NK	NK
AN18892 (B4871)	M	31	Autism	99	1600	Left	Gun shot	No	No	NK	NK	NK	NK
AN09901 (B5764)	M	32	Autism	28.65	1694	Right	Heat shock	No	No	NK	NK	NK	NK
AN06746 (B4541)	M	44	Autism	30.8	1530	NK	Cardiac arrest	No	No	NK	NK	NK	NK
AN19534 (B6143)	M	45	Autism	40.16	1360	Right	Aspiration	Yes	No	4	NA	14	27
AN18838 (B6202)	M	48	Autism	NK	1260	Right	Asphyxia	No	Yes	8	NA	14	29

NK, not known; NA, not applicable.

from the Autism Tissue Program (ATP) and the UC Davis Medical Center. The autistic cases were all diagnosed as classical autism. The diagnosis of autism was confirmed by standard postmortem use of the autism diagnostic interview-revised (ADI-R) in all cases. The control cases were determined to be free of neurological disorders, including autism, based on medical records and information gathered at the time of death from next of kin. Cases were all males, except for 1 control case. Age, hemisphere, brain weight, severity of symptoms, and postmortem interval varied from case to case (Table 1). Control cases averaged 32.2 years with a range of 6–56 years. Autism cases averaged 26.5 with a range of 7–48 years. Two of the subjects with autism suffered from seizures and 3 from mental retardation (Table 1). Control patients did not have a history of seizures, mental retardation, or dementia.

Based on Brodmann cortical neuroanatomy, we isolated a block containing BA9 in the superior PFC, BA46 in the middle PFC, and BA47 in the inferior PFC, from each case (Fig. 1A). We cut the tissue into 14 µm sections on a cryostat, stained 1 section with Nissl (Fig. 1D), and based on cytoarchitecture selected the region in each section that matched the von Economo description for BA9 (F_{Dm}), BA46 ($F_{D\Delta}$), and BA47 (Ffα). See "Anatomical and cytoarchitectural considerations" in Methods (Fig. 1B). We used thin-cut slices of 14 µm to obtain a single layer of cells for quantification. A single cell layer avoids overlapping cells and reduces quantification errors, such as counting 2 overlapping cells as only one cell. In addition, thin-cut sections allowed us to obtain more sections per block of tissue to increase data yield for additional experiments. This is very important since there is a severe lack of tissue from autism subjects currently available for research.

Since we had access to small blocks of tissue that did not encompass entire BAs, we could not apply stereological methods. We therefore used an approach based on quantifying total interneuron cell number in 3 mm wide bins that encompassed the entire thickness of the cortical gray matter within representative samples of each BA. Within each selected BA of interest, we chose a bin that was 3 mm wide that extended from the pial surface through the thickness of the gray matter to include all cortical layers (Fig. 1C). To ensure that we obtained representative samples of interneuron populations in each Brodmann area, we ran replication studies to quantify interneuron cell number in a second 3 mm bin selected from a different region of each BA (Fig. 1C). As in the primary study, bins in the replication study were selected in Nissl-stained sections (Fig. 1C). For both primary and replication studies, we performed triple immunostaining for PV, CB, and CR using Nova Red (pink), DAB (brown), and Vector Blue (blue) substrates to identify immunolabeled cells on sections that were directly adjacent to the Nissl-stained sections. We quantified and compared the number of interneuron types in the primary and replication study and found that interneuron number and percentages did not differ between studies within each BA for each case, indicating that the selected region to study was representative of each BA as a whole.

We used monoclonal antibodies for PV and CB, and a polyclonal antibody for CR for our analysis. To test the specificity of these antibodies, we ran a validation study and compared the immunostaining we obtained in tissue sections of control BA46, BA47, and BA9 tissue with that produced by a second set of anti-PV, CB, and CR antibodies. The second set of antibodies included polyclonal PV and CB antibodies, and a monoclonal CR antibody. We compared results obtained from the first and second sets of antibodies by quantifying the number of PV+, CR+, and CB+ cells in bins from 3 slices of PFC from 3 cases. We compared the number of immunopositive cells obtained with the first and second sets of antibodies and found essentially the same number of interneurons, supporting the specificity of the antibodies chosen for the experimental work.

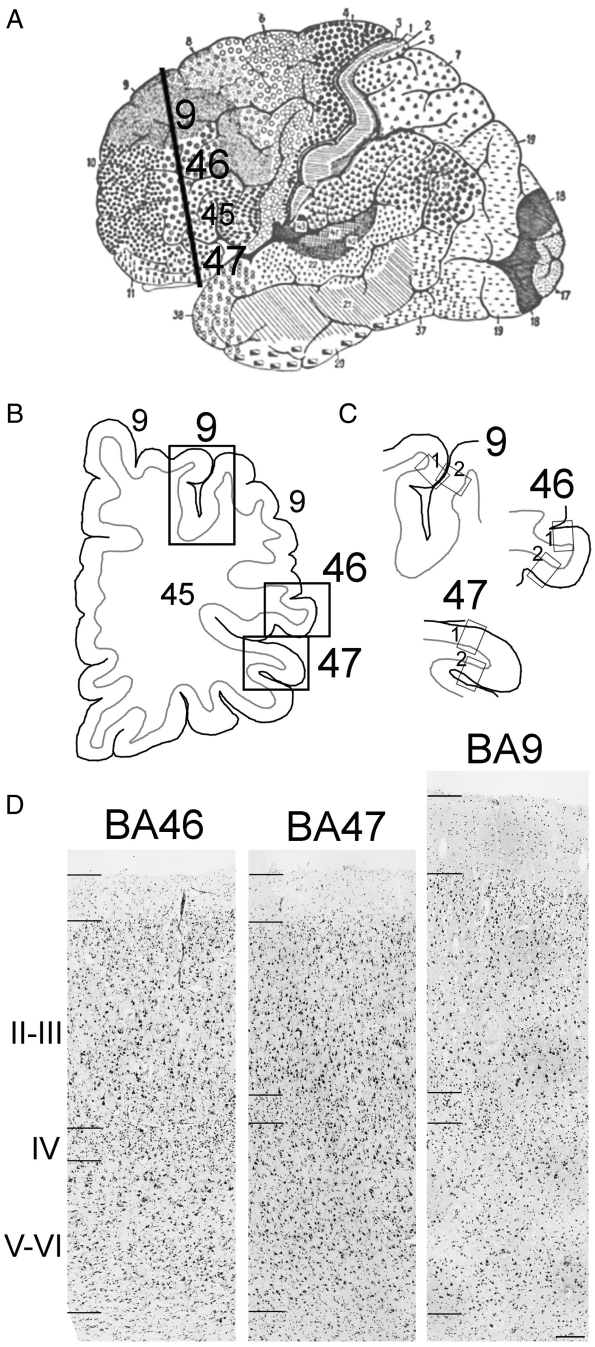

Figure 1. Cortical areas investigated in this study. Blocks of prefrontal cortical tissue containing BA9, BA46, and BA47 were isolated based on Brodmann and von Economo analysis. The cytoarchitectonic region that exactly matched the von Economo description for cortical areas (BA9/FDm; BA46/FDΔ; and BA47/Ffα) was selected in coronal sections prepared from each case. (*A*) Brodmann areas in the cerebral cortex. The line represents the plane of sectioning used to obtain cortical sections. (*B*) A line drawing of a coronal section used in this study. Brodmann areas 9, 46, and 47 are indicated with black boxes. (*C*) Regions of Brodmann areas 9, 46, and 47 analyzed in the primary and replication studies are indicated with "box 1" and "box 2" in each BA. (*D*) Nissl-stained sections of areas BA46, BA47, and BA9. Hash marks on the left side of each image demark boundaries of Layer 1, the supragranular layers, Layer IV, and the infragranular layers and the white matter. Scale bar in *D*: 200 µm.

Once we had validated our method and the antibodies, we performed triple immunostaining for PV, CB, and CR and counterstained the tissue with Nissl substance to label the nuclei of all neurons and glia and the soma of all neurons in all the autism cases and all the control cases. We quantified the number of PV+ (pink), CB+ (brown), and CR+ (blue) cells, and of double and triple-labeled cells for each marker within the area of interest (Fig. 2). We compared the number of each cell type in autism and control cases. One of the autism cases (20 years old) was not analyzed for BA47 due to histological abnormalities. The number of double-labeled cells was minimal across subjects, <1% of interneurons in each area (Fig. 3*D*).

Using light microscopy with a ×100 lens, we quantified the total number of each interneuron subtype within each bin and

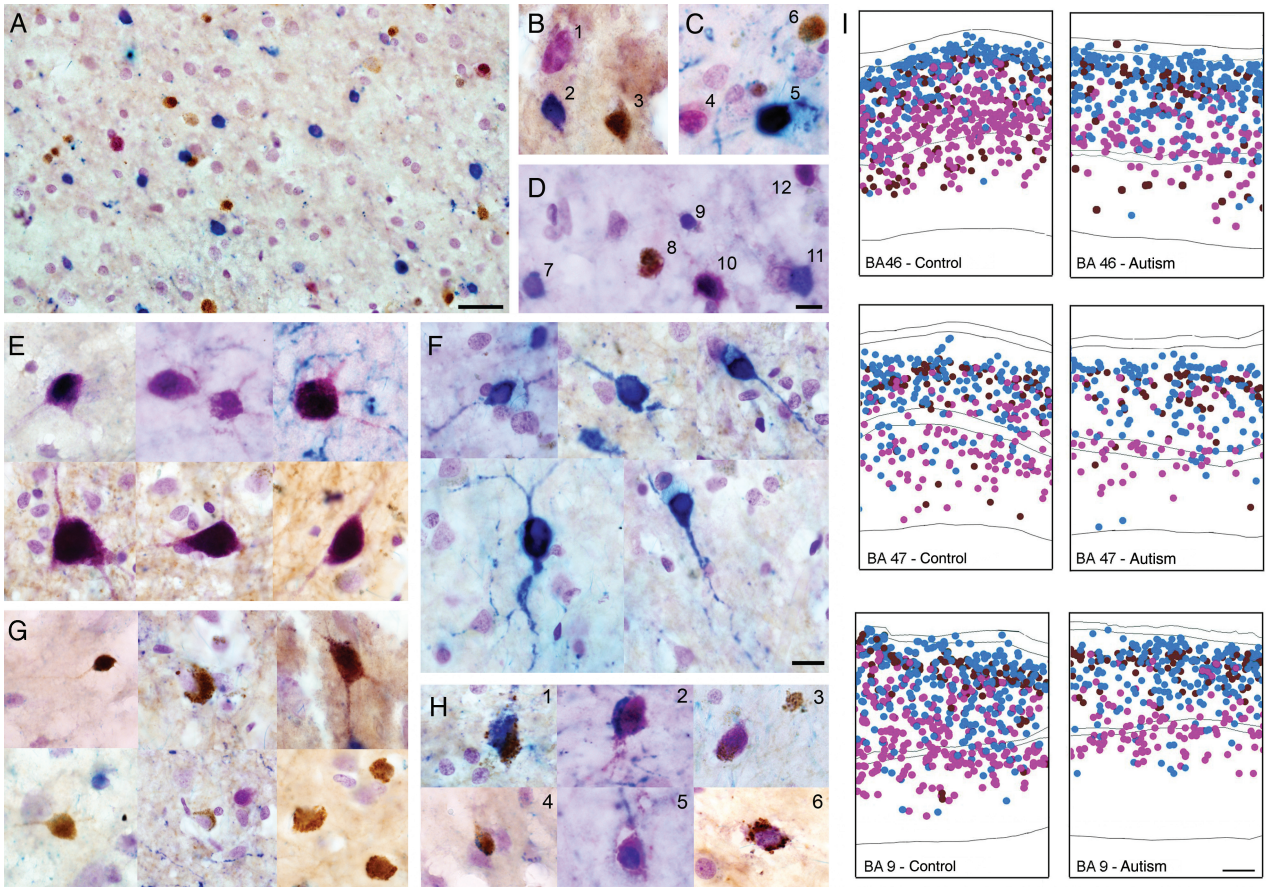

Figure 2. Image showing a section of prefrontal cerebral cortex triple immunostained with antibodies against PV (pink), CR (blue), CB (brown), and counterstained with Nissl. (*A*) Image showing clear differentiation of PV (dark pink/violet), CR (blue), CB (brown) labeled interneurons and Nissl-stained cells (light purple). (*B–D*) High-power magnification image showing labeled PV+ interneurons (dark pink: 1, 4, 10); CR+ interneurons (blue: 2, 5, 7, 9, 11); and CB+ interneurons (brown: 3, 6, 8). (*E*) PV+ interneurons (dark pink). (*F*) CR+ interneurons (blue). (*G*) CB+ interneurons (brown). (*H1–H6*) Examples of double immunolabeled interneurons: 1, CR+/CB+ (blue/brown); 2, CR+/PV+ (blue/dark pink); 3, CB+/PV+ (brown/dark pink); 4, CR+/CB+ (blue/brown); 5, CR+/PV+ (blue/dark pink); 6, CB+/PV+ (brown/dark pink). (*I*) Representative diagrams depicting the location of PV+ interneurons (pink), CR+ interneurons (blue), and CB+ interneurons (brown) in bins from autistic and control cases in each BA. Scale bar in *A* = 100 µm, in *D* (*B–D*) = 25 µm, In *F* (*E–H*): 25 µm, *I* = 250 µm.

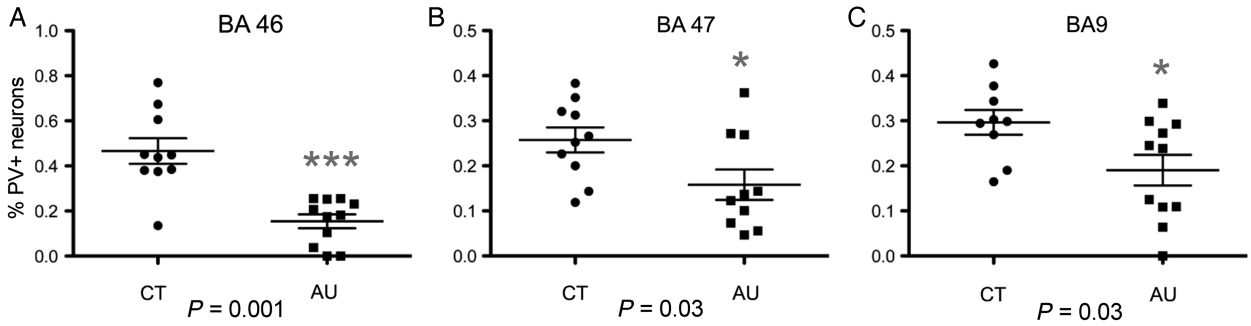

Figure 3. Percentage of parvalbumin+ (PV+) cells in Brodmann areas (BA) 46, 47, and 9 in autistic (AU) and control (CT) brains. The percentage of PV+ cells in autistic cases was significantly lower in BA46, BA47, and BA9 than in control cases. The degree of significance is indicated with asterisks: ***$P < 0.001$; *$P < 0.05$.

each case. Then we calculated the percentage of each interneuron subtype out of the total number of interneurons for each bin. We defined the total number of interneurons as equal to the sum of all PV+, CR+, and PV+ interneurons. Quantifying the number of interneuron subtypes as a percentage avoids the introduction of error due to differential tissue shrinkage that occurs in each case and which can alter cell density measurements. In BA46, we counted an average of 286.0 ± 35.4$^{(SEM)}$ PV+, CB+, and CR+ immunolabeled cells per case (range of 141–640 cells per case). In BA47, we counted an average of 366.15 ± 34.2 immunolabeled cells per case (range of 162–759). In BA9, we counted an average of 336.2 ± 28.6 immunolabeled cells per case (range of 94–626 cells per case).

Compared with control cases, the autistic cases exhibited a significant decrease in the percentage of PV+ interneurons in each cortical area examined, but there was no change in the percentage of CR+ or CB+ interneurons (Fig. 4 and see Supplementary Table 1). In BA46, the percentage of PV+ cells was decreased by nearly 70% in autism cases compared with controls: 50.3 ± 5%$^{(SEM)}$ of all interneurons were PV+ in CT cases versus 15.4 ± 3% in AU cases ($P = 0.0001$). The proportion of CB+ and CR+ cells did not differ in BA46 (CB+ cells: 22.3 ± 2% in CT vs. 34.3 ± 5% in AU, $P = 0.53$; CR+ cells: 15.5 ± 4% in CT vs. 27.6 ± 5% in AU, $P = 0.60$). Similarly, in BA47, we found that the percentage of PV+ interneurons was significantly reduced by 38% in autism: 25.7 ± 2% of all interneurons were PV+ in CT versus 15.8 ± 3% in AU ($P = 0.03$). The percentage of CB+ and CR+ cells in BA47 did not differ between control and autism cases (CB+ cells: 31.7 ± 2% in CT vs. 31.0 ± 2% in AU, $P = 0.84$; CR+ cells: 47.6 ± 3% in CT vs. 52.7 ± 3% in AU, $P = 0.32$). In BA9, we also found a significant decrease in the percentage of PV+ interneurons of 45%: 29.6 ± 2% of all interneurons were PV+ in CT versus 19.0 ± 3% in

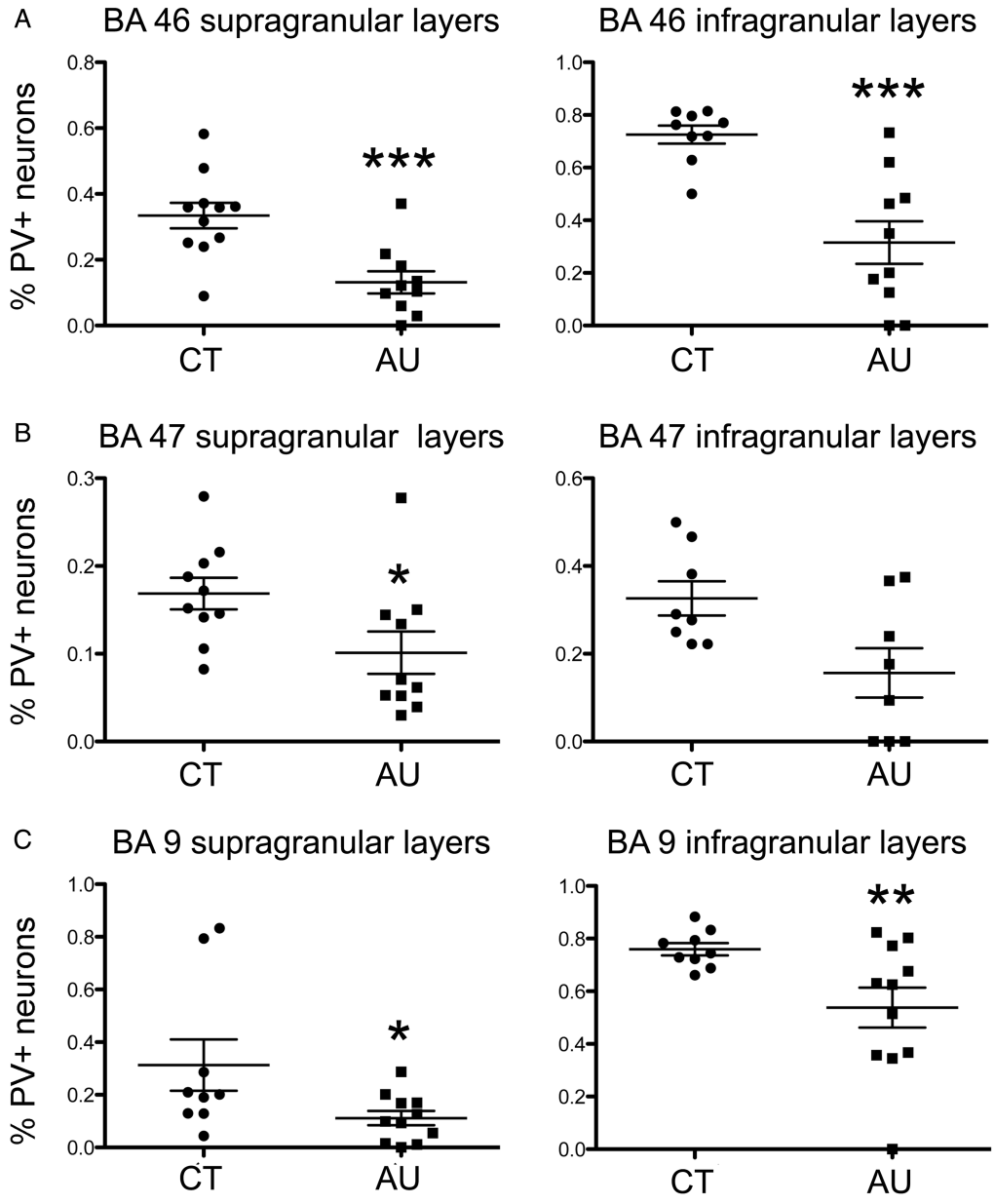

Figure 4. The percentage of parvalbumin+ (PV+) cells was significantly lower in both supragranular and infragranular layers in Brodmann areas (BA)46, BA47, and BA9 of autism cases (AU) than in control cases (CT). The degree of significance is indicated with asterisks: ***$P < 0.001$; **$P < 0.01$; *$P < 0.05$.

AU ($P = 0.03$). The percentage of CB+ and CR+ cells did not differ between controls and autism cases in BA9 (CB+ cells: 17.0 ± 4% in CT vs. 18.7 ± 2% in AU, $P = 0.50$; CR+ cells: 53.3 ± 8% in CT vs. 61.6 ± 4% in AU, $P = 0.13$, Fig. 3 and see Supplementary Table 1).

PV+ cells were not present in BA46 in 2 cases, and PV+ cells were not present in 1 case in BA9. However, in these cases, PV+ cells were present in the other BAs analyzed, suggesting that this was not an artifact of staining. However, we repeated the statistical analyses after eliminating these cases and found a statistically significant difference in the number of PV+ cells between autism and control group (BA46: $P = 0.004$; BA9: $P = 0.05$). We also performed statistical analysis after removing the 2 autistic cases with seizures included in this study and obtained a similar result in the 3 PFC areas: a significant decrease in the percentage of PV+ interneurons (always $P < 0.05$), but no change in the percentage of CB+ and CR+ interneurons (always $P > 0.1$).

We performed correlation analyses of the percentage of each interneuronal subpopulation with a set of case variables and found no correlation of the percentage of PV+ interneurons to any of these variables (Age: $R = 0.30$, $P = 0.18$; brain weight: $R = 0.04$; $P = 0.84$; right or left hemisphere: $R = 0.05$, $P = 0.84$; mental retardation: $R = 0.14$, $P = 0.65$; PMI: $R = 0.19$, $P = 0.45$). Supplementary Figure 2 shows the correlation obtained for number of PV+ cells and age. We could not correlate quantification results with the presence of seizures since only 2 cases presented with this feature. We performed intra- and inter-rater analysis for quantification in the 3 BAs, and in all cases, these variables did not significantly differ ($P > 0.1$).

We tested our quantification approach by analyzing a second 3-mm-wide bin within each Brodmann area for all the control and autism cases (Fig. 1C). We obtained the same result showing a significant decrease in the percentage of PV+ interneurons (see Supplementary Table 2). These data support our finding that the number of PV+ cells is decreased within BA46, BA47, and BA9. In our repeat analysis, we noticed an increase in the percentage of CR+ cells in BA47 and BA9, which we interpret as a potential compensation for the decrease in the percentage of PV+ interneurons.

We next tested whether the decreased percentage of PV+ neurons resulted primarily from a decrease of PV+ cell number that was specific to the supragranular or infragranular layers. We delineated supragranular (II–III) and infragranular (V–VI) layers based on the Nissl counterstaining of the tissue and quantified the percentage of interneuron subtypes as above. We found that the reduction in the percentage of PV+ interneurons occurred equally in supra- and infragranular layers (Fig. 4 and see Supplementary Tables 3–5). In BA46, the percentage of PV+ interneurons in the supragranular layers of the autism group was reduced 70% compared with control cases (33 ± 4% of all interneurons were PV+ in CT vs. 11 ± 3% in AU, $P = 0.0004$). In BA47, the percentage of PV+ cells in the supragranular layers was reduced 38% in autism cases (16 ± 1% of all interneurons were PV+ in CT vs. 10 ± 2% in AU, $P = 0.03$). In BA9, the percentage of PV+ interneurons was reduced 73% in the supragranular layers of autism cases (31 ± 9% of all interneurons were PV+ in CT vs. 11 ± 2% in AU, $P = 0.04$). Thus, the reduction of PV+ interneurons in the supragranular layers was significant in all 3 prefrontal area quantified.

The reduction of PV+ interneurons in the infragranular layers was significant in BA46 and B9, and reduced in BA47, but not quite significant. In BA46, the percentage of PV+ interneurons in the infragranular layers of the autism group was reduced 55% compared with control cases (71 ± 3% of all interneurons were PV+ in CT vs. 32 ± 7% in AU, $P = 0.0001$). In BA47, the percentage of PV+ interneurons was reduced 25% in the infragranular layers, although this decrease was not fully significant (60 ± 5% of all interneurons were PV+ in CT vs. 45 ± 8% in AU, $P = 0.15$). In BA9, the percentage of PV+ interneurons was reduced 30% in the infragranular layers (75 ± 2% of all interneurons were PV+ in CT vs. 53 ± 7% in AU, $P = 0.01$).

Methods

Subjects

We collected prefrontal BA9, BA46, and BA47 in samples obtained from 11 autism and 10 control, age-matched cases (Table 1). The tissue was obtained from the Autism Tissue Program (ATP) and the UC Davis Medical Center. The autistic cases were all diagnosed as classical autism. The diagnosis of autism was confirmed by standard postmortem use of the autism diagnostic interview-revised (ADI-R) in all cases. The control cases were determined to be free of neurological disorders, including autism, based on medical records and information gathered at the time of death from next of kin. Cases were all males, except for one control case.

Immunostaining

We performed enzymatic staining on postmortem human tissue, which has several advantages over immunofluorescent staining. Fluorescent staining of human tissue can often produce false positives, requires fluorescent microscopy to analyze, and the signal fades over time. In contrast, enzymatic staining is not subjected to the autofluorescence that occurs in poorly fixed, non-perfused human tissue with long postmortem intervals, it can be analyzed with light microscopy, and the stained tissue is preserved for future analysis. To set up the staining protocol, we first performed single staining with each marker and then triple staining using all possible combinations of antibodies and substrates. We quantified immunopositive cells for each marker in the single staining and in each of the protocols for triple staining, and chose the protocol that produced the most accurate quantification for each interneuron marker. For these preliminary experiments, we compared the number of each cell type using each protocol and chose the optimal protocol that produced the highest number of cells for each marker that did not differ statistically from the number of cells produced in single immunostaining experiments for each marker. We determined that the combination of CB-brown, CR-blue, and PV-red was best for distinguishing interneuron subpopulations (see Supplementary Fig. 1).

We used the following primary antibodies for our quantification experiments: monoclonal mouse anti-CB-D28k (1:500, Swant 300, Switzerland), polyclonal rabbit anti-CR (1:500, Swant 7697), and monoclonal mouse anti-PV (1:500, Swant 235). The following primary antibodies were used for our validation study: polyclonal rabbit anti-CB (1:500, Abcam ab11426), monoclonal mouse anti-CR (1:500, Millipore mab1568), and polyclonal rabbit anti-PV (1:500, Abcam ab11427). Secondary antibodies were donkey anti-mouse conjugated with biotin, amplified with avidin-biotin complex (ABC) and developed with diaminobenzidine (DAB) or Vector NovaRED substrates (all from Vector, USA) for CB and PV detection, respectively. Donkey anti-rabbit antibody conjugated with alkaline phosphatase and Vector Blue substrate (Vector) was used for CR detection. Tissue was pretreated in Diva decloaker (DV2004 LX, MX, Biocare medical, USA) in a decloaking chamber (Biocare medical, USA) at 110°C for 6 min. Subsequently, immunostained tissues were immersed in 0.1% Nissl for 1 min

and then dehydrated in successive baths of 50% ethanol (30 s), 70% ethanol (30 s), 95% ethanol (10 min), and 100% ethanol (5 min), isopropanol (5 min) followed by 15 min in xylene solution, mounted, and cover-slipped with Permount (Fisher). The PV-red staining usually developed into a red pigment, but following Nissl staining, it was visualized as pink.

Anatomical and Cytoarchitectural Considerations

Based on Brodmann cortical neuroanatomy, blocks containing area BA9 in the superior PFC, BA46 in the middle PFC, and BA47 in the inferior PFC, were isolated from each case. Anatomical dissection of the blocks was performed at the ATP by qualified staff. We cut 14-µm sections on a cryostat, stained 1 section with Nissl, and based on von Economo cytoarchitecture selected the region in each section that exactly matched the von Economo descriptions for each area (see below). On adjacent sections we performed triple immunostaining for PV, CB, and CR.

Anatomy

BA9 (magnocellular granular frontal area, or F_{Dm} of von Economo) consists of a strip-like zone whose medial boundary is the callosomarginal sulcus and its ventral boundary is the inferior frontal sulcus. BA 46 (middle granular frontal area, or $F_{D\Delta}$ of von Economo) includes the middle third of the middle and the most anterior part of the inferior frontal gyri at the transition to the orbital surface. BA47 (orbital area, or $F_{F}\alpha$ of von Economo) surrounds the posterior branches of the orbital sulcus and laterally crosses the orbital part of the inferior frontal gyrus (Brodmann 1909).

Cytoarchitecture

BA9 and BA45 surround BA46. In BA46, cortical layers are more differentiated than those in BA9, particularly at the borders of Layer IV. Layers III and V exhibit a clear sublamination in BA9, but not in BA46. Neurons in BA46 are more homogeneous in size than those in BA9. For example, the density of cells is greater in Layer IIIa of BA9 (32 000 cells/m^3) than in Layer IIIb (16 000 cells/mm^3), being neurons larger in IIIb (15–40 µm height). In contrast, Layer III neurons in BA46 have a homogenous density (32 500 cells/mm^3) and smaller cell size (20–30 µm height). In addition, BA9 has different cell density in Va1 (35 000 cells/mm^3), Va2 (20 000 cells/mm^3), and Vb (12 000 cells/mm^3) with the largest cells in Vb (20–40 µm). In contrast, cell density is homogenous in Layer V of BA46 (30 000 cells/mm^3). In brief, BA9 is characterized by the presence of large pyramidal cells in sublayers IIIc and Va1, a pale violet-stained sublayer Vb, and a narrow and indistinct Layer IV. The transition area BA9–46 contains cytoarchitectonic features of both BA9 and 46. Like BA9, BA46 is characterized by relatively low cell-packing density and a violet-pale sublayer Vb. The portion of BA9 on the middle frontal gyrus can be discriminated from the surrounding areas by the presence of large, violet deeply stained pyramidal neurons in the lower half of Layer III. In contrast, BA46 has a Layer III that contains small to medium size pyramidal neurons, giving it a rather uniform appearance. BA45 and BA11 surround BA47. BA45 contains a violet-pale sublayer Vb (12 000 cells/mm^3), while BA47 Layer Vb has a higher cell density (30 000 cells/mm^3). BA45 has large and packed pyramidal cells in Layer IIIc, which is replaced by small and medium cells in BA47. BA11 lacks internal granular layer (IV), has small size neuronal cell bodies in all layers, a non-differentiated Layers I–II, and lacks a clear border between Layers II and III and between Layer VI and white matter (von Economo 1929).

Quantification

We stained 1 section of each case (11 autistic cases and 10 control cases) in each BA with Nissl. In the Nissl-stained section, we selected the region in each section that exactly matched the von Economo description for that BA. Within selected regions of interest, we chose a 3-mm wide bin parallel to the pial surface and that extended perpendicular from the pia through the thickness of the cortical gray matter to include all cortical layers. We used a ×100 oil objective on a microscope (Olympus BX61 microscope with a Hamamatsu Camera, a Dell Precision PWS 690, Intel Xeon CPU Computer with Microsoft Windows XP Professional V.2002 system, and MBF Bioscience StereoInvestigator V.9 Software, MicroBrightField, Williston, VT). We quantified the number of immunopositive cells for each interneuron subtype (CB+, CR+, or PV+ cells). Cell identification was based on the screen image of each cell and corroboration through the microscope oculars. We counted as positive those cell that had immunostaining within the cytoplasm. We did not quantify any cells that appeared to have immunopositive processes or perisomatic staining but that lacked cytoplasmic immunolabeling. We excluded a small number of immunopositive cells from our analysis (<0.01% of cells) that we identified as pyramidal neurons based on their morphology in Nissl counterstaining. The total number of interneurons was quantified by summing CB+, CR+, and PV+ interneurons.

Statistics

The goal of the statistical analysis was to compare percentage of each type of interneuron between autistic and control cases, and to assess the relationship between anatomical parameters and other patient/sample characteristics (such as age, hemisphere, presence of mental retardation or seizures and severity of autism) in autistic cases and overall. The percentage of each type of interneuron was compared between autistic and control cases using *t*-tests. The joint influence of autism and patient/sample characteristics on variables was assessed using multiple regression modeling, with regression models chosen using stepwise selection.

Discussion

Despite the long-held concept that an imbalance in the ratio of excitation to inhibition might underlie the cognitive phenotype in some forms of ASD (Rubenstein and Merzenich 2003), a quantification of the number of interneurons in distinct areas of the cerebral cortex of autistic subjects had not yet been carried out. We addressed this gap in knowledge by quantifying the percentage of 3 main subtypes of cortical interneurons, PV+, CB+, and CR+ cells, in 3 areas of the PFC that have been implicated in autism: BA46, BA47, and BA9. Here we report that the percentage of PV+ interneurons is reduced in the 3 areas of the autistic PFC that we examined, while the percentage of CB+ interneurons and CR+ interneurons was not significantly altered.

The only related data we are aware of in the literature is that by Zikopoulos and Barbas (2013), who examined PV+ and CB+ neurons in postmortem BA9 tissue from subjects with ASD ($n = 2$ ASD, 30 and 44 years, and $n = 2$ controls), and found a decrease in the ratio of PV to CB inhibitory neurons in autism (Zikopoulos and Barbas 2013). Our data obtained from 11 autism subjects and 10 control cases match their data, and also that obtained from experiments in some mouse models of autism. For example, experiments in mice showed that misexpression of Fmr1, a protein affected in Fragile X (Lozano et al. 2014) produced a significant reduction in the density of PV+ interneurons (20%, $P < 0.001$), but not CB+ and CR+ interneurons (Selby et al. 2007).

Our data differ from that reported by Lawrence et al. (2010) in a study of interneuron subpopulations in the human hippocampus of autistic subjects. They reported an increase in the density of CB+ interneurons in the dentate gyrus, an increase in CR+ interneurons in CA1, and an increase in PV+ interneurons in areas CA1 and CA3 in individuals with autism compared with controls (Lawrence et al. 2010). However, the hippocampus and neocortex have distinct structural and functional properties, and therefore, we did not predict similar alterations in the number or percentage of specific neuronal subtypes in the autistic cerebral cortex. In line with our present results, several mouse models of human disease present with a reduced number of interneurons in various brain regions. For example, a deficiency of the Disc1 gene in mice, which is correlated with some cases of autism (Kilpinen et al. 2008; Lim et al. 2009; Williams et al. 2009; Crepel et al. 2010; Zheng et al. 2011), produced a significant reduction of PV+ interneurons in the hippocampus (Nakai et al. 2014). Engrailed 2 (En2) is a candidate gene for ASDs (Gharani et al. 2004; Benayed et al. 2005; Wang et al. 2008; Sen et al. 2010) and En2(−/−) mice presented with a reduction of PV+ interneurons in both the cerebral cortex and hippocampus (Sgado et al. 2013). Mouse models that produce deficits in other genes associated with autism, including MeCP2 and Neuroligin 3, also present with cortical interneuron defects (Tabuchi et al. 2007; Tomassy et al. 2014). Thus, gene deficits associated with some cases of ASD appear to produce alterations in interneuron subpopulations that are similar to the decreased numbers of PV+ interneurons we find in the PFC of individuals with autism.

Interneuron subtypes in the cerebral cortex exhibit distinct morphological and physiological properties and connectivity patterns. Each interneuron subtype modulates the activity of excitatory cortical cells through different mechanisms. PV antibodies label 2 principle subtypes of interneurons, basket cells (Bs) and the chandelier cells (Ch). These 2 interneuron subtypes synthesize and release GABA, and generate fast-spiking action potentials that synchronize the activity of numerous pyramidal cells through rhythmic inhibition (Kawaguchi et al. 1987; Kawaguchi and Kubota 1997; Goldman-Rakic 1999; Markram et al. 2004; Woodruff et al. 2009). PV+ interneurons are the primary interneurons in the cortex that directly innervate the soma or initial segment of the pyramidal neuron axon (Somogyi 1977; DeFelipe and Gonzalez-Albo 1998). In contrast, CB+ and CR+ interneurons innervate the distal dendritic arbor of pyramidal neurons.

Basket cells are multipolar PV+ interneurons located throughout Layers II–VI that establish multiple connections with the soma and proximal dendrites of pyramidal neurons in a manner that outlines the pyramidal cell body giving it a basket-like shape. Basket cells are subdivided into small, large, and nest basket cells, that present with differential size, dendritic and axonal projections, firing properties, and the expression of additional molecular markers (Kawaguchi and Kubota 1997; Wang et al. 2002; Goldberg et al. 2008). Parvalbumin+ Ch cell interneurons are mainly distributed between Layers III and VI. The terminal portions of PV+ Ch cell axons form vertical rows of synaptic boutons that resemble a candlestick and are called cartridges (Szentagothai and Arbib 1974; DeFelipe et al. 1985). Each Ch cell has multiple cartridges, and each cartridge innervates the initial segment of a single pyramidal neuron axon. Each Ch cell therefore regulates the output of many pyramidal neurons. Several studies have suggested that a subgroup of Ch cells may be excitatory rather than inhibitory (Szabadics et al. 2006; Khirug et al. 2008), but recent experiments using noninvasive approaches have found no evidence for depolarizing effects of Ch cells (Glickfeld et al. 2009; Woodruff et al. 2010). Each PV+ cell, whether a Bs or Ch cell, innervates a large number of pyramidal neurons; therefore, the loss of even a small number of PV+ cells could critically impair pyramidal neuron output and regional cortical function (DeFelipe 1999). In addition to PV+ Bs and Ch cells, multipolar bursting cells at the interface of Layers I–II in mouse cortex have been described to express PV, but differ from Bs and Ch cells in their electrophysiological properties and connectivity (Blatow et al. 2003). Further studies in postmortem tissue of subjects with autism are needed to discern whether all PV+ interneurons or rather a specific subtype of PV+ interneuron is affected in autism. Nevertheless, because of the unique connectional properties of PV+ interneurons, a deficit in the number of any subtype of PV+ could alter inhibition of pyramidal neurons and cortical functioning.

EEG recordings of the human cortex show several distinct patterns of oscillations that represent different brain activity states. Oscillatory fluctuations across time are representative of communication events between different cell types in the cortex (Buzsaki et al. 2012). Specifically, gamma oscillations result from the interaction between synaptic excitation produced by glutamatergic neurons and inhibition produced by GABAergic neurons. When pyramidal neurons are released from the inhibition exerted by Bs and/or Ch cells, they fire in concert and the repetition of this cycle provides a synchronized oscillation of a neuronal network at a frequency that is inversely related to the duration of the pyramidal neuron inhibition (Gonzalez-Burgos and Lewis 2008). It has been hypothesized that PV+ interneurons are responsible for the generation of gamma oscillations through their perisomatic and axo-axonic inhibition and therefore control the timing of spike discharges of pyramidal neurons (Whittington et al. 1995, 2011; Bartos et al. 2007; Buzsaki and Wang 2012). In agreement with this, several recent studies have shown that inhibition of PV+ interneurons in the cortex suppressed gamma oscillations in vivo (Cardin et al. 2009; Sohal et al. 2009). It has also been proposed that gamma oscillations could be a physiological biomarker for abnormality of PV+ neurons (Nakamura et al. 2015). Therefore, understanding the number and distribution of PV+ interneurons in the autistic cerebral cortex may shed light on the nature of cortical functioning in some cases of autism.

We recognize that a decrease in the number of PV-expressing cells would not necessarily result from a decreased number of neurons, but could also result from decreased PV protein expression by those cells. Recently, a PV knockout mouse has been shown to display behavioral phenotypes with relevance to all 3 core symptoms present in human ASD patients, including abnormal reciprocal social interactions, impairments in communication, and repetitive and stereotyped patterns of behavior. These mice also showed several signs of ASD-associated comorbidities, including increased susceptibility to seizures. Reduced social interactions and communication were also observed in heterozygous mice characterized by lower PV expression levels, indicating that merely a decrease in PV levels might be sufficient to elicit core ASD-like deficits (Wohr et al. 2015). PV plays a role in short-term synaptic plasticity. Indeed, in PV knockout mice, synapses with short-term depression are converted to synapses with short-term facilitation resulting in enhanced synaptic transmission (Caillard et al. 2000). On the other hand, the loss of Bs and/or Ch cells in the autistic cortex would likely translate into decreased inhibition of pyramidal neuron output, and the loss of inhibitory synapses could cause hyperexcitation of the cortical synaptic circuits. Therefore, both phenomena, a decrease in the number of PV+ cells or a decrease in PV expression

by these interneurons, could alter pyramidal neuron inhibition and consequently synaptic transmission in the autistic cerebral cortex.

Changes in morphology and/or function of PV+ Bs cells and PV + Ch cells have previously been reported in neurological diseases, such as schizophrenia and epilepsy (Woo et al. 1998; Defelipe et al. 1999; Pierri et al. 1999; Volk and Lewis 2002; Volk et al. 2002; Lewis et al. 2012). Glausier and colleagues quantified PV+ basket cell inputs in BA9 of schizophrenic and matched control subjects and found that the levels of PV protein were lower in PV+ basket boutons in schizophrenia (Glausier et al. 2014). Woo et al. (1998) found that the density of PV+ Ch cell cartridges was decreased by 40% in the PFC of schizophrenic subjects compared with matched groups of normal control and nonschizophrenic psychiatric subjects. The changes in PV+ interneurons reported in these cases may reflect altered information processing within the PFC and could contribute to the shared cognitive and genetic impairments seen in schizophrenia and epilepsy (Woo et al. 1998).

The prefrontal areas included in this study regulate aspects related to memory, verbal, and auditory functions. A decrease in the number of PV+ interneurons in any of these cortical areas could impact these cognitive functions, as is seen in patients with autism. The decrease in the proportion of PV+ cell varied across the cortical areas we studied, ranging from 70% in BA46 to 38% in BA47. This difference may be related to the fact that the number of PV-expressing interneurons varies across prefrontal cortical areas in the control cortex. For example, 50.3% of the interneurons were PV+ in BA46 of control brains, while only 25.7% were PV+ in BA47, and 29.6% in BA9 of control brains. Our observation that BA46, BA47, and BA9 prefrontal areas exhibit a decreased number of PV+ cells presents the question whether alterations in the number or proportion of interneuron are also present in other prefrontal and nonprefrontal areas of the cerebral cortex in autism. More studies are needed to investigate this matter in autism.

The decrease in PV+ cells we found in the PFC in autism could be an underlying cause of cognitive and behavioral symptoms in autism. On the other hand since PV expression is influenced by activity, decreased numbers of PV-expressing cells could be a consequence of the symptoms. Variables such as medications, the presence of seizures, or insults to the brain could also influence PV+ cell numbers.

The discovery that PV+ interneurons are reduced in the autistic cerebral cortex suggests a possible deficit of inhibition on pyramidal neurons. More studies are needed to achieve a fuller understanding of the cellular basis of autism. Establishing the underlying mechanisms at play in autism will be essential for the development of new therapeutic interventions.

Supplementary Material

Supplementary material can be found at: http://www.cercor.oxfordjournals.org/.

Funding

This work was supported by the National Institute for Mental Health (MH094681 and MH101188), the MIND Institute (IDDRC; U54 HD079125), the Shriners Hospitals, and the Pathology Department at UCD.

Notes

Tissue was obtained from Autism BrainNet that is sponsored by the Simons Foundation and Autism Speaks. The authors also acknowledge the Autism Tissue Program that was the predecessor to Autism BrainNet. Also, E.H. was partially supported by an Autism Science Foundation fellowship. *Conflict of Interest*: None declared.

Authors' contributions

E.H. collaborated in protocol design and writing of the manuscript and acquired data; J.A. collaborated in protocol design and data acquisition, and took images; H.R. collaborated in data acquisition; S.N. collaborated in study design and writing of the manuscript; V.M.-C. designed the study, analyzed, and interpreted data, made figures, wrote the manuscript, and supervised study.

References

Baio J. 2012. Prevalence of autism spectrum disorders - autism and developmental disabilities monitoring network, 14 sites, United States, 2008. CDC MMWR Surv Summ. 61:1–19.

Bartos M, Vida I, Jonas P. 2007. Synaptic mechanisms of synchronized gamma oscillations in inhibitory interneuron networks. Nat Rev Neurosci. 8:45–56.

Belmonte MK, Yurgelun-Todd DA. 2003. Functional anatomy of impaired selective attention and compensatory processing in autism. Brain Res Cogn Brain Res. 17:651–664.

Benayed R, Gharani N, Rossman I, Mancuso V, Lazar G, Kamdar S, Bruse SE, Tischfield S, Smith BJ, Zimmerman RA, et al. 2005. Support for the homeobox transcription factor gene ENGRAILED 2 as an autism spectrum disorder susceptibility locus. Am J Hum Genet. 77:851–868.

Blatow M, Rozov A, Katona I, Hormuzdi SG, Meyer AH, Whittington MA, Caputi A, Monyer H. 2003. A novel network of multipolar bursting interneurons generates theta frequency oscillations in neocortex. Neuron. 38:805–817.

Brodmann K. 1909. Vergleichende Lokalisationslehre der Grobhirnrinde. Leipzig: Verlag von Johann Ambrosius Barth.

Brown C, Gruber T, Boucher J, Rippon G, Brock J. 2005. Gamma abnormalities during perception of illusory figures in autism. Cortex. 41:364–376.

Buzsaki G, Anastassiou CA, Koch C. 2012. The origin of extracellular fields and currents—EEG, ECoG, LFP and spikes. Nat Rev Neurosci. 13:407–420.

Buzsaki G, Wang XJ. 2012. Mechanisms of gamma oscillations. Annu Rev Neurosci. 35:203–225.

Caillard O, Moreno H, Schwaller B, Llano I, Celio MR, Marty A. 2000. Role of the calcium-binding protein parvalbumin in short-term synaptic plasticity. Proc Natl Acad Sci USA. 97:13372–13377.

Camacho J, Ejaz E, Ariza J, Noctor SC, Martinez-Cerdeno V. 2014. RELN-expressing neuron density in layer I of the superior temporal lobe is similar in human brains with autism and in age-matched controls. Neurosci Lett. 579C:163–167.

Cardin JA, Carlen M, Meletis K, Knoblich U, Zhang F, Deisseroth K, Tsai LH, Moore CI. 2009. Driving fast-spiking cells induces gamma rhythm and controls sensory responses. Nature. 459:663–667.

Casanova MF, Buxhoeveden DP, Brown C. 2002. Clinical and macroscopic correlates of minicolumnar pathology in autism. J Child Neurol. 17:692–695.

Casanova MF, El-Baz A, Vanbogaert E, Narahari P, Switala A. 2010. A topographic study of minicolumnar core width by lamina comparison between autistic subjects and controls: possible minicolumnar disruption due to an anatomical

element in-common to multiple laminae. Brain Pathol. 20:451–458.
Cauli B, Audinat E, Lambolez B, Angulo MC, Ropert N, Tsuzuki K, Hestrin S, Rossier J. 1997. Molecular and physiological diversity of cortical nonpyramidal cells. J Neurosci. 17: 3894–3906.
Cline H. 2005. Synaptogenesis: a balancing act between excitation and inhibition. Curr Biol. 15:R203–R205.
Cobos I, Calcagnotto ME, Vilaythong AJ, Thwin MT, Noebels JL, Baraban SC, Rubenstein JL. 2005. Mice lacking Dlx1 show subtype-specific loss of interneurons, reduced inhibition and epilepsy. Nat Neurosci. 8:1059–1068.
Cohen MX, David N, Vogeley K, Elger CE. 2009. Gamma-band activity in the human superior temporal sulcus during mentalizing from nonverbal social cues. Psychophysiology. 46:43–51.
Conde F, Lund JS, Jacobowitz DM, Baimbridge KG, Lewis DA. 1994. Local circuit neurons immunoreactive for calretinin, calbindin D-28k or parvalbumin in monkey prefrontal cortex: distribution and morphology. J Comp Neurol. 341:95–116.
Courchesne E, Mouton PR, Calhoun ME, Semendeferi K, Ahrens-Barbeau C, Hallet MJ, Barnes CC, Pierce K. 2011. Neuron number and size in prefrontal cortex of children with autism. JAMA. 306:2001–2010.
Crepel A, Breckpot J, Fryns JP, De la Marche W, Steyaert J, Devriendt K, Peeters H. 2010. DISC1 duplication in two brothers with autism and mild mental retardation. Clin Genet. 77:389–394.
Dani VS, Chang Q, Maffei A, Turrigiano GG, Jaenisch R, Nelson SB. 2005. Reduced cortical activity due to a shift in the balance between excitation and inhibition in a mouse model of Rett syndrome. Proc Natl Acad Sci USA. 102:12560–12565.
DeFelipe J. 1999. Chandelier cells and epilepsy. Brain. 122(Pt 10): 1807–1822.
DeFelipe J. 1997. Types of neurons, synaptic connections and chemical characteristics of cells immunoreactive for calbindin-D28K, parvalbumin and calretinin in the neocortex. J Chem Neuroanat. 14:1–19.
DeFelipe J, Gonzalez-Albo MC. 1998. Chandelier cell axons are immunoreactive for GAT-1 in the human neocortex. Neuroreport. 9:467–470.
Defelipe J, Gonzalez-Albo MC, Del Rio MR, Elston GN. 1999. Distribution and patterns of connectivity of interneurons containing calbindin, calretinin, and parvalbumin in visual areas of the occipital and temporal lobes of the macaque monkey. J Comp Neurol. 412:515–526.
DeFelipe J, Hendry SH, Jones EG, Schmechel D. 1985. Variability in the terminations of GABAergic chandelier cell axons on initial segments of pyramidal cell axons in the monkey sensory-motor cortex. J Comp Neurol. 231:364–384.
DeFelipe J, Lopez-Cruz PL, Benavides-Piccione R, Bielza C, Larranaga P, Anderson S, Burkhalter A, Cauli B, Fairen A, Feldmeyer D, et al. 2013. New insights into the classification and nomenclature of cortical GABAergic interneurons. Nat Rev Neurosci. 14:202–216.
del Rio MR, DeFelipe J. 1997. Colocalization of parvalbumin and calbindin D-28k in neurons including chandelier cells of the human temporal neocortex. J Chem Neuroanat. 12:165–173.
Dixon ML, Christoff K. 2014. The lateral prefrontal cortex and complex value-based learning and decision making. Neurosci Biobehav Rev. 45:9–18.
Dumontheil I. 2014. Development of abstract thinking during childhood and adolescence: the role of rostrolateral prefrontal cortex. Dev Cogn Neurosci. 10:57–76.
Dumontheil I, Burgess PW, Blakemore SJ. 2008. Development of rostral prefrontal cortex and cognitive and behavioural disorders. Dev Med Child Neurol. 50:168–181.
Fatemi SH, Halt AR, Realmuto G, Earle J, Kist DA, Thuras P, Merz A. 2002. Purkinje cell size is reduced in cerebellum of patients with autism. Cell Mol Neurobiol. 22:171–175.
Francis A, Msall M, Obringer E, Kelley K. 2013. Children with autism spectrum disorder and epilepsy. Pediatr Ann. 42:255–260.
Gharani N, Benayed R, Mancuso V, Brzustowicz LM, Millonig JH. 2004. Association of the homeobox transcription factor, ENGRAILED 2, 3, with autism spectrum disorder. Mol Psychiatry. 9:474–484.
Glausier JR, Fish KN, Lewis DA. 2014. Altered parvalbumin basket cell inputs in the dorsolateral prefrontal cortex of schizophrenia subjects. Mol Psychiatry. 19:30–36.
Glickfeld LL, Roberts JD, Somogyi P, Scanziani M. 2009. Interneurons hyperpolarize pyramidal cells along their entire somatodendritic axis. Nat Neurosci. 12:21–23.
Goldberg EM, Clark BD, Zagha E, Nahmani M, Erisir A, Rudy B. 2008. K+ channels at the axon initial segment dampen near-threshold excitability of neocortical fast-spiking GABAergic interneurons. Neuron. 58:387–400.
Goldman-Rakic PS. 1999. The "psychic" neuron of the cerebral cortex. Ann N Y Acad Sci. 868:13–26.
Gonzalez-Burgos G, Lewis DA. 2008. GABA neurons and the mechanisms of network oscillations: implications for understanding cortical dysfunction in schizophrenia. Schizophr Bull. 34:944–961.
Helmeke C, Ovtscharoff W Jr, Poeggel G, Braun K. 2008. Imbalance of immunohistochemically characterized interneuron populations in the adolescent and adult rodent medial prefrontal cortex after repeated exposure to neonatal separation stress. Neuroscience. 152:18–28.
Hof PR, Glezer II, Conde F, Flagg RA, Rubin MB, Nimchinsky EA, Vogt Weisenhorn DM. 1999. Cellular distribution of the calcium-binding proteins parvalbumin, calbindin, and calretinin in the neocortex of mammals: phylogenetic and developmental patterns. J Chem Neuroanat. 16:77–116.
Jeon HA. 2014. Hierarchical processing in the prefrontal cortex in a variety of cognitive domains. Front Syst Neurosci. 8:223.
Kawaguchi Y, Katsumaru H, Kosaka T, Heizmann CW, Hama K. 1987. Fast spiking cells in rat hippocampus (CA1 region) contain the calcium-binding protein parvalbumin. Brain Res. 416:369–374.
Kawaguchi Y, Kubota Y. 1997. GABAergic cell subtypes and their synaptic connections in rat frontal cortex. Cereb Cortex. 7:476–486.
Kennedy DP, Semendeferi K, Courchesne E. 2007. No reduction of spindle neuron number in frontoinsular cortex in autism. Brain Cogn. 64:124–129.
Khirug S, Yamada J, Afzalov R, Voipio J, Khiroug L, Kaila K. 2008. GABAergic depolarization of the axon initial segment in cortical principal neurons is caused by the Na-K-2Cl cotransporter NKCC1. J Neurosci. 28:4635–4639.
Kilpinen H, Ylisaukko-Oja T, Hennah W, Palo OM, Varilo T, Vanhala R, Nieminen-von Wendt T, von Wendt L, Paunio T, Peltonen L. 2008. Association of DISC1 with autism and Asperger syndrome. Mol Psychiatry. 13:187–196.
Kim E, Camacho J, Combs Z, Ariza J, Lechpammer M, Noctor SC, Martinez-Cerdeno V. 2015. Preliminary findings suggest the number and volume of supragranular and infragranular pyramidal neurons are similar in the anterior superior temporal area of control subjects and subjects with autism. Neurosci Lett. 589:98–103.

Kubota Y, Hattori R, Yui Y. 1994. Three distinct subpopulations of GABAergic neurons in rat frontal agranular cortex. Brain Res. 649:159–173.

Kuchukhidze G, Wieselthaler-Holzl A, Drexel M, Unterberger I, Luef G, Ortler M, Becker AJ, Trinka E, Sperk G. 2015. Calcium-binding proteins in focal cortical dysplasia. Epilepsia. 56:1207–1216.

Lawrence YA, Kemper TL, Bauman ML, Blatt GJ. 2010. Parvalbumin-, calbindin-, and calretinin-immunoreactive hippocampal interneuron density in autism. Acta Neurol Scand. 121:99–108.

Leuba G, Saini K. 1997. Colocalization of parvalbumin, calretinin and calbindin D-28k in human cortical and subcortical visual structures. J Chem Neuroanat. 13:41–52.

Levisohn PM. 2007. The autism-epilepsy connection. Epilepsia. 48 (Suppl. 9):33–35.

Lewis DA, Curley AA, Glausier JR, Volk DW. 2012. Cortical parvalbumin interneurons and cognitive dysfunction in schizophrenia. Trends Neurosci. 35:57–67.

Lim SM, Kim HJ, Nam M, Chung JH, Park YH. 2009. Association study of DISC1 in Korean population with autism spectrum disorders. Psychiatr Genet. 19:160.

Lozano R, Rosero CA, Hagerman RJ. 2014. Fragile X spectrum disorders. Intract Rare Dis Res. 3:134–146.

Mandy W, Lai MC. 2016. Annual Research Review: The role of the environment in the developmental psychopathology of autism spectrum condition. J Child Psychol Psychiatry. 57(3):271–292.

Markram H, Toledo-Rodriguez M, Wang Y, Gupta A, Silberberg G, Wu C. 2004. Interneurons of the neocortical inhibitory system. Nat Rev Neurosci. 5:793–807.

Martínez-Cerdeño V, Camacho J, Fox V, Miller E, Ariza J, Kienzle D, Plank K, Noctor SC, Van de Water J. 2016. Prenatal exposure to autism-specific maternal autoantibodies alters proliferation of cortical neural precursor cells, enlarges brain, and increases neuronal size in adult animals. Cereb Cortex. 26(1): 374–383.

Milne E, Scope A, Pascalis O, Buckley D, Makeig S. 2009. Independent component analysis reveals atypical electroencephalographic activity during visual perception in individuals with autism. Biol Psychiatry. 65:22–30.

Mukaetova-Ladinska EB, Arnold H, Jaros E, Perry R, Perry E. 2004. Depletion of MAP2 expression and laminar cytoarchitectonic changes in dorsolateral prefrontal cortex in adult autistic individuals. Neuropathol Appl Neurobiol. 30:615–623.

Nakai T, Nagai T, Wang R, Yamada S, Kuroda K, Kaibuchi K, Yamada K. 2014. Alterations of GABAergic and dopaminergic systems in mutant mice with disruption of exons 2 and 3 of the Disc1 gene. Neurochem Int. 74:74–83.

Nakamura T, Matsumoto J, Takamura Y, Ishii Y, Sasahara M, Ono T, Nishijo H. 2015. Relationships among parvalbumin-immunoreactive neuron density, phase-locked gamma oscillations, and autistic/schizophrenic symptoms in PDGFR-beta knock-out and control mice. PLoS One. 10: e0119258.

Nassar M, Simonnet J, Lofredi R, Cohen I, Savary E, Yanagawa Y, Miles R, Fricker D. 2015. Diversity and overlap of parvalbumin and somatostatin expressing interneurons in mouse presubiculum. Front Neural Circuits. 9:20.

Oberman LM, Hubbard EM, McCleery JP, Altschuler EL, Ramachandran VS, Pineda JA. 2005. EEG evidence for mirror neuron dysfunction in autism spectrum disorders. Brain Res Cogn Brain Res. 24:190–198.

Orekhova EV, Stroganova TA, Nygren G, Tsetlin MM, Posikera IN, Gillberg C, Elam M. 2007. Excess of high frequency electroencephalogram oscillations in boys with autism. Biol Psychiatry. 62:1022–1029.

Pierri JN, Chaudry AS, Woo TU, Lewis DA. 1999. Alterations in chandelier neuron axon terminals in the prefrontal cortex of schizophrenic subjects. Am J Psychiatry. 156:1709–1719.

Polleux F, Lauder JM. 2004. Toward a developmental neurobiology of autism. Ment Retard Dev Disabil Res Rev. 10:303–317.

Romanski LM. 2007. Representation and integration of auditory and visual stimuli in the primate ventral lateral prefrontal cortex. Cereb Cortex. 17(Suppl. 1):i61–i69.

Rubenstein JL. 2010. Three hypotheses for developmental defects that may underlie some forms of autism spectrum disorder. Curr Opin Neurol. 23:118–123.

Rubenstein JL, Merzenich MM. 2003. Model of autism: increased ratio of excitation/inhibition in key neural systems. Genes Brain Behav. 2:255–267.

Russo N, Zecker S, Trommer B, Chen J, Kraus N. 2009. Effects of background noise on cortical encoding of speech in autism spectrum disorders. J Autism Dev Disord. 39:1185–1196.

Santos M, Uppal N, Butti C, Wicinski B, Schmeidler J, Giannakopoulos P, Heinsen H, Schmitz C, Hof PR. 2011. Von Economo neurons in autism: a stereologic study of the frontoinsular cortex in children. Brain Res. 1380:206–217.

Schaefer GB. 2016. Clinical genetic aspects of ASD spectrum disorders. Int J Mol Sci. 17(2):180.

Schumann CM, Amaral DG. 2006. Stereological analysis of amygdala neuron number in autism. J Neurosci. 26:7674–7679.

Schumann CM, Amaral DG. 2005. Stereological estimation of the number of neurons in the human amygdaloid complex. J Comp Neurol. 491:320–329.

Selby L, Zhang C, Sun QQ. 2007. Major defects in neocortical GABAergic inhibitory circuits in mice lacking the fragile X mental retardation protein. Neurosci Lett. 412:227–232.

Sen B, Singh AS, Sinha S, Chatterjee A, Ahmed S, Ghosh S, Usha R. 2010. Family-based studies indicate association of Engrailed 2 gene with autism in an Indian population. Genes Brain Behav. 9:248–255.

Sgado P, Genovesi S, Kalinovsky A, Zunino G, Macchi F, Allegra M, Murenu E, Provenzano G, Tripathi PP, Casarosa S, et al. 2013. Loss of GABAergic neurons in the hippocampus and cerebral cortex of Engrailed-2 null mutant mice: implications for autism spectrum disorders. Exp Neurol. 247:496–505.

Shalom DB. 2009. The medial prefrontal cortex and integration in autism. Neuroscientist. 15:589–598.

Skefos J, Cummings C, Enzer K, Holiday J, Weed K, Levy E, Yuce T, Kemper T, Bauman M. 2014. Regional alterations in purkinje cell density in patients with autism. PLoS One. 9:e81255.

Sohal VS, Zhang F, Yizhar O, Deisseroth K. 2009. Parvalbumin neurons and gamma rhythms enhance cortical circuit performance. Nature. 459:698–702.

Somogyi P. 1977. A specific 'axo-axonal' interneuron in the visual cortex of the rat. Brain Res. 136:345–350.

Szabadics J, Varga C, Molnar G, Olah S, Barzo P, Tamas G. 2006. Excitatory effect of GABAergic axo-axonic cells in cortical microcircuits. Science. 311:233–235.

Szentagothai J, Arbib MA. 1974. Conceptual models of neural organization. Neurosci Res Prog Bull. 12:305–510.

Tabuchi K, Blundell J, Etherton MR, Hammer RE, Liu X, Powell CM, Sudhof TC. 2007. A neuroligin-3 mutation implicated in autism increases inhibitory synaptic transmission in mice. Science. 318:71–76.

Teffer K, Semendeferi K. 2012. Human prefrontal cortex: evolution, development, and pathology. Prog Brain Res. 195:191–218.

Thatcher RW, North DM, Neubrander J, Biver CJ, Cutler S, Defina P. 2009. Autism and EEG phase reset: deficient GABA mediated inhibition in thalamo-cortical circuits. Dev Neuropsychol. 34:780–800.

Tomassy GS, Morello N, Calcagno E, Giustetto M. 2014. Developmental abnormalities of cortical interneurons precede symptoms onset in a mouse model of Rett syndrome. J Neurochem. 131:115–127.

Uppal N, Gianatiempo I, Wicinski B, Schmeidler J, Heinsen H, Schmitz C, Buxbaum JD, Hof PR. 2014. Neuropathology of the posteroinferior occipitotemporal gyrus in children with autism. Mol Autism. 5:17.

van Kooten IA, Palmen SJ, von Cappeln P, Steinbusch HW, Korr H, Heinsen H, Hof PR, van Engeland H, Schmitz C. 2008. Neurons in the fusiform gyrus are fewer and smaller in autism. Brain. 131:987–999.

Volk DW, Lewis DA. 2002. Impaired prefrontal inhibition in schizophrenia: relevance for cognitive dysfunction. Physiol Behav. 77:501–505.

Volk DW, Pierri JN, Fritschy JM, Auh S, Sampson AR, Lewis DA. 2002. Reciprocal alterations in pre- and postsynaptic inhibitory markers at chandelier cell inputs to pyramidal neurons in schizophrenia. Cereb Cortex. 12:1063–1070.

von Economo C. 1929. The cytoarchitectonics of the human cerebral cortex. London: Humphrey Milford - Oxford University.

Wang L, Jia M, Yue W, Tang F, Qu M, Ruan Y, Lu T, Zhang H, Yan H, Liu J, et al. 2008. Association of the ENGRAILED 2 (EN2) gene with autism in Chinese Han population. Am J Med Genet B Neuropsychiatr Genet. 147B:434–438.

Wang Y, Gupta A, Toledo-Rodriguez M, Wu CZ, Markram H. 2002. Anatomical, physiological, molecular and circuit properties of nest basket cells in the developing somatosensory cortex. Cereb Cortex. 12:395–410.

Wegiel J, Flory M, Kuchna I, Nowicki K, Ma SY, Imaki H, Wegiel J, Cohen IL, London E, Wisniewski T, et al. 2014. Stereological study of the neuronal number and volume of 38 brain subdivisions of subjects diagnosed with autism reveals significant alterations restricted to the striatum, amygdala and cerebellum. Acta Neuropathol Commun. 2:141.

Whitney ER, Kemper TL, Bauman ML, Rosene DL, Blatt GJ. 2008. Cerebellar Purkinje cells are reduced in a subpopulation of autistic brains: a stereological experiment using calbindin-D28k. Cerebellum. 7:406–416.

Whitney ER, Kemper TL, Rosene DL, Bauman ML, Blatt GJ. 2009. Density of cerebellar basket and stellate cells in autism: evidence for a late developmental loss of Purkinje cells. J Neurosci Res. 87:2245–2254.

Whittington MA, Cunningham MO, LeBeau FE, Racca C, Traub RD. 2011. Multiple origins of the cortical gamma rhythm. Dev Neurobiol. 71:92–106.

Whittington MA, Traub RD, Jefferys JG. 1995. Synchronized oscillations in interneuron networks driven by metabotropic glutamate receptor activation. Nature. 373:612–615.

Williams JM, Beck TF, Pearson DM, Proud MB, Cheung SW, Scott DA. 2009. A 1q42 deletion involving DISC1, DISC2, and TSNAX in an autism spectrum disorder. Am J Med Genet A. 149A: 1758–1762.

Wohr M, Orduz D, Gregory P, Moreno H, Khan U, Vorckel KJ, Wolfer DP, Welzl H, Gall D, Schiffmann SN, et al. 2015. Lack of parvalbumin in mice leads to behavioral deficits relevant to all human autism core symptoms and related neural morphofunctional abnormalities. Transl Psychiatry. 5:e525.

Woo TU, Whitehead RE, Melchitzky DS, Lewis DA. 1998. A subclass of prefrontal gamma-aminobutyric acid axon terminals are selectively altered in schizophrenia. Proc Natl Acad Sci USA. 95:5341–5346.

Woodruff A, Xu Q, Anderson SA, Yuste R. 2009. Depolarizing effect of neocortical chandelier neurons. Front Neural Circuits. 3:15.

Woodruff AR, Anderson SA, Yuste R. 2010. The enigmatic function of chandelier cells. Front Neurosci. 4:201.

Zheng F, Wang L, Jia M, Yue W, Ruan Y, Lu T, Liu J, Li J, Zhang D. 2011. Evidence for association between Disrupted-in-Schizophrenia 1 (DISC1) gene polymorphisms and autism in Chinese Han population: a family-based association study. Behav Brain Funct. 7:14.

Zikopoulos B, Barbas H. 2013. Altered neural connectivity in excitatory and inhibitory cortical circuits in autism. Front Hum Neurosci. 7:609.